DALTON
FULL PAPER

Crystal structures and magnetic properties of the interpenetrating rutile-related compounds $M(tcm)_2$ [M = octahedral, divalent metal; tcm^- = tricyanomethanide, $C(CN)_3^-$] and the sheet structures of $[M(tcm)_2(EtOH)_2]$ (M = Co or Ni)

Stuart R. Batten,[ab] Bernard F. Hoskins,[a] Boujemaa Moubaraki,[b] Keith S. Murray *[b] and Richard Robson *[a]

[a] *School of Chemistry, University of Melbourne, Parkville, Victoria 3052, Australia. E-mail: r.robson@chemistry.unimelb.edu.au*
[b] *Department of Chemistry, Monash University, Clayton, Victoria 3168, Australia*

Received 2nd June 1999, Accepted 29th June 1999

The isomorphous structures of $M(tcm)_2$ [M^{II} = Cr, Mn, Fe, Co, Ni, Cu, Zn, Cd or Hg; tcm^- = tricyanomethanide, $C(CN)_3^-$] contain two interpenetrating rutile-related networks generated by octahedral six-connecting metal ions and trigonal three-connecting tcm^- anions. The detailed variable temperature and variable field magnetic properties of this series of high-spin complexes generally point to the existence of very weak intraframework coupling with no evidence for long range magnetic order or interframework effects. The compound $Cr(tcm)_2$ is the most strongly coupled and displays a field independent maximum in susceptibility at 14.5 K and a J value of -1.6 cm^{-1} (using a $-2JS_1 \cdot S_2$ Heisenberg chain model); $Co(tcm)_2$ displays high temperature magnetic moments typical of essentially uncoupled octahedral centres but with a most unusual field dependence in μ_{Co} observed below 10 K, probably due to very weak ferromagnetic coupling, and an M_{sat} value in high fields, at 2 K, which is significantly less than that expected for $S = 3/2$. Doping of $M(tcm)_2$ with another M′ member of the series leads to a crystal structure isomorphous with $M(tcm)_2$ in which the dopant metal M′ occupies the M site in a random fashion. The resultant magnetism is simply intermediate between those of the parent phases. The isomorphous structures of $[M(tcm)_2(EtOH)_2]$ (M^{II} = Co or Ni) contain pseudo square-grid sheets in which the tcm^- ligands are each co-ordinated to two metal ions and act as a kinked bridge. Each metal is co-ordinated to four tcm^- anions in an equatorial arrangement and to two axial ethanol ligands. Extensive intrasheet hydrogen bonding exists between the ethanol molecules and the unco-ordinated nitrile of the tcm^- bridges.

We[1] and others[2] are interested in the construction of new co-ordination polymers whose structures are governed by the topological properties of the precursor metal ions and ligands. It is hoped that by judicious choice of ligand and metal connectivity we can control the topology and geometry of the network formed, and possibly the physical properties of the resultant compounds. Such crystal engineering may afford new materials with useful properties such as catalytic activity, microporosity, non-linear optical activity and co-operative magnetic behaviour.

The most common approach by far has been the combination of linear 2-connecting ligands with metal ions of varying connectivity. For example, the use of linear connecting ligands and 4-connecting tetrahedral metal ions usually results in the formation of diamond-related networks. Linear connecting ligands and 6-connecting octahedral metal centres can result in co-ordination polymers with α-Po-like topology.

Networks formed by ligands with connectivities higher than two have been less studied. Moore and co-workers[3] have produced a number of interesting co-ordination polymers using trigonal 3-connecting ligands, as have a number of other groups[4] including ours. The trigonal 3-connecting ligands 2,4,6-tri(4-pyridyl)triazine[5] and 1,4,5,8,9,12-hexaazatriphenylene[6] afford co-ordination polymers generally of high symmetry with a wide range of topologies and geometries which in a number of cases are without precedent. Metal derivatives of a relatively small number of 4-connecting ligands have also been explored, some with tetrahedral geometry[1a,7] and others square planar.[8]

One of the simplest possible 3-connecting ligands is the tricyanomethanide ion (tcm^-, $C(CN)_3^-$, **1**), whose internal stability is reflected in the fact that its conjugate acid, $HC(CN)_3$, is a very strong acid ($pK_a \approx -5$).[9,10] Cox and Fontaine[11] reported the synthesis of K(tcm) and Ag(tcm) in 1954, while Middleton and co-workers reported $Ba(tcm)_2$[12] as part of a seminal series of papers on cyanocarbons from the laboratories of Du Pont.[13] Subsequently various metal derivatives of tcm^- were studied by Kohler and co-workers.[14] Crystal structure studies of simple salts of tcm^- with NH_4^+,[15] Na^+[16] and K^+[17] and of other derivatives involving either unco-ordinated[18] or monodentate[19] tcm^- generally reveal an essentially planar tcm^-; one notable exception is $[Ir(CO)(tcm)(PPh_3)_2]$, which shows a distortion towards pyramidal geometry.[20]

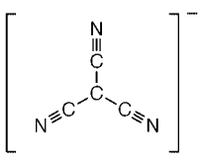

The anion tcm^- appeared to offer considerable promise as a building block for infinite co-ordination networks because it is robust, stable under a variety of conditions, easily synthesized as a variety of salts,[21] its planar, trigonal geometry appears to be fairly rigid, and it co-ordinates to metal centres readily on account of its negative charge and good terminal nitrogen donors. We have already reported a range of new co-ordination polymers in which both tcm^- and various co-ligands act simultaneously as connecting units. The compound Ag(tcm)

Table 1 Cell parameters, calculated and experimental densities for $M(tcm)_2$

Metal	a/Å	b/Å	c/Å	V/Å^3	D_c/g cm^{-3}	D_e/g cm^{-3}
Cr	7.330(1)	5.545(1)	10.743(2)	431.9(2)	1.784	1.770(3)
Mn	7.660(1)	5.372(1)	10.603(3)	436.3(3)	1.789	1.799(5)
Co	7.474(1)	5.241(1)	10.432(2)	408.6(2)	1.943	1.971(5)
Ni	7.366(1)	5.2266(6)	10.368(2)	399.2(2)	1.987	2.000(5)
Cu	7.168(1)	5.4680(6)	10.764(1)	421.9(1)	1.918	1.935(5)
Zn	7.466(2)	5.3171(5)	10.482(2)	416.1(2)	1.960	1.988(10)
Cd	7.828(2)	5.4677(8)	10.7378(7)	459.6(2)	2.114	2.146(5)
Hg	7.833(2)	5.535(1)	10.759(2)	466.4(2)	2.710	2.730(3)
Co/Cu	7.363(1)	5.302(1)	10.492(2)	409.6(1)	1.975	—
Mn/Co	7.489(9)	5.240(4)	10.460(5)	410.5(6)	1.922	—

Space group *Pmna* (no. 53).

contains layers of doubly interpenetrating (6,3) sheets,[22,23] while analogous double layers in $[Ag(tcm)(phenz)_{0.5}]$ are bridged by the phenazine (phenz) ligands to give two interpenetrating 3-D networks.[23] Two interpenetrating 3-D networks are also seen in the structure of [Ag(tcm)(pyz)] (pyz = pyrazine), although they have different topology to those seen in the phenazine compound.[23] The compound $[Cd(tcm)(B(OMe)_4)]\cdot x$MeOH has a chiral 3-D network in which the tcm^- acts as a 3-connecting unit and the bridging/chelating $B(OMe)_4^-$ effectively acts as a linear 2-connector,[24] [Cd(tcm)(hmt)(H_2O)][tcm] (hmt = hexamethylenetetramine) forms a rutile-related network held together by both co-ordinate and hydrogen bonds,[25] [Cu(tcm)(hmt)], [Cu(tcm)(bipy)] (bipy = 4,4′-bipyridine) and [Cu(tcm)(bpe)]·0.25bpe·0.5MeCN [bpe = 1,2-bis(4-pyridyl)ethene] have (4,4) sheet structures displaying interdigitation, interpenetration and intercalation, respectively.[26] Reports of a number of other polymeric tcm^- structures have also appeared, some including studies of magnetic properties.[27]

The simple "binary" compounds $M(tcm)_2$ (M^{II} = Fe, Cu, Co, Ni or Mn) were first reported by Trofimenko *et al.*[28] Very shortly afterwards Enemark and Holm[29] reported similar results. The compound $Cr(tcm)_2$ was reported in 1968,[30] and Kohler and co-workers[31] studied various spectroscopic properties of these compounds. Before our work, however, the only reported crystal structure of these derivatives was that of $Cu(tcm)_2$ in a preliminary communication by Biondi *et al.*[32] in 1965 which proved to be misleading, with the interpenetrating networks not commented upon.

The work reported here also forms part of a study we are undertaking on the structural and magnetic properties of the co-ordination polymers of the less-common pseudohalide ligands. One particular aim of this study is to obtain new molecular magnets, which undergo a magnetic phase transition to an ordered state at the Curie temperature T_c (ferromagnet) or the Neel temperature T_N (antiferromagnet). Most such magnetic materials contain two different d-block metal ions, or different oxidation states of the same ion such as in the Prussian-blue like phases containing the well studied pseudohalide bridging group CN^-.[33–35] Other well studied pseudohalide bridged systems containing N_3^- or NCS^- have received a lot of magnetochemical attention although few compounds have displayed long range order, two recent exceptions being some homometallic manganese(II)[36] and cobalt(II) species.[37]

We[38] and others[39] have been studying the structural and magnetochemistry of metal derivatives of the dicyanamide anion, $N(CN)_2^-$ (dca^-, **2**), a close relative of tcm^-. The structures of $M(dca)_2$ (M^{II} = Mn, Fe, Co, Ni or Cu) are isomorphous and contain rutile-like co-ordination networks, with octahedral M centres and 3-connecting dca^- ligands (*via* all three nitrogen donors).[38,39] The magnetic properties of these dca^- complexes vary widely, depending on the metal: Cu^{II} (d^9) is a paramagnet, Ni^{II} (d^8) and Co^{II} (d^7) are ferromagnets (T_c = 9 and 20 K, respectively) and Fe^{II} (d^6) and Mn^{II} (d^5) are canted antiferromagnets (T_N = 19 and 16 K, respectively). We have also studied a number of co-ordination polymers of dca^- containing bridging co-ligands such as pyrazine and 4,4′-bipyridine.[38]

We described the interpenetrating structure of $Zn(tcm)_2$ in 1991,[40] and in the same year reported the isomorphous structures[1c,5a,41] of a number of other metal derivatives that we now present in full below. More recently we have determined their magnetic properties,[25,38a,b] which are also presented in full below. Very recently, Miller and co-workers[42] reported the crystal structure and magnetic properties of $Mn(tcm)_2$.

Included in the present report are the synthesis and structures of alcohol-solvated forms of the "binary" compounds $[M(tcm)_2(EtOH)_2]$ which were obtained from alcohol solution in the same way as the unsolvated $M(tcm)_2$ derivatives from aqueous solution. A similar critical dependence of structure upon reaction medium is also seen when the series of $M(dca)_2$ derivatives are obtained from various solvents.[38]

Results and discussion

Crystal structures

$M(tcm)_2$. All members of the $M(tcm)_2$ series (M^{II} = Cr, Mn, Fe, Co, Ni, Cu, Zn, Cd or Hg) are isomorphous, possessing similar cell parameters and identical space group (*Pmna*). Complete structure solutions for the derivatives of Cr, Cu, Zn and Hg based on single crystal diffraction data were carried out. The derivatives of Mn, Co, Ni and Cd were shown to be isomorphous on the basis of cell parameters and space group, also obtained by single crystal measurements, whilst powder diffraction was used to demonstrate that the iron derivative is isomorphous with the others. The cell parameters are summarised in Table 1.

For M = Cr, Cu, Zn, Hg selected bond lengths and angles are shown in Table 2. The structures consist of two interpenetrating rutile-related networks. Each of the two identical networks consists of six-connecting centres (octahedral metal ions) and three-connecting centres (tcm^- ligands) in the ratio 1:2, with a topology identical to that of rutile (Fig. 1). The rutile topology is becoming an increasingly common one in crystal engineering,[25,38,39] although an alternative topology for a 3,6-connected net has been reported.[5d]

In the rutile prototype (TiO_2), the separation between the 3- and 6-connecting nodes of the network is just the Ti–O distance (1.946(3) and 1.984(4) Å).[43] In $M(tcm)_2$, however, this separation is the considerably larger C–C–N–M distance, *ca.* 4.5–5.0 Å. This results in a much more spacious structure that allows a second framework to interpenetrate the first, as shown schematically in Fig. 1(b). Interestingly, in the $M(dca)_2$ compounds described earlier, which have only a single rutile-like network, two of the connections between 3- and 6-connecting nodes are of the N–C–N–M type and are similar in length to the C–C–N–M connections in the $M(tcm)_2$ derivatives. The third connection, however, is of the considerably shorter direct

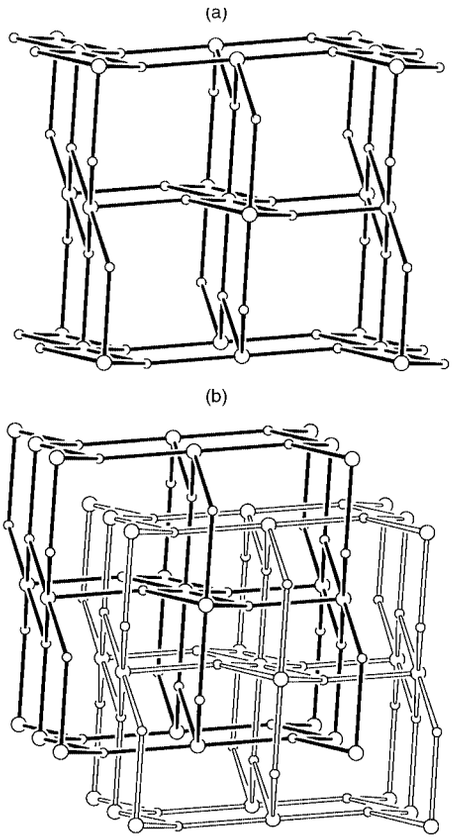

Fig. 1 (a) A single rutile-like framework in $M(tcm)_2$. Only the metal atoms and central carbon atoms of the tcm^- anion are shown. The bonds represent C–C≡N–M linkages. (b) Two interpenetrating frameworks.

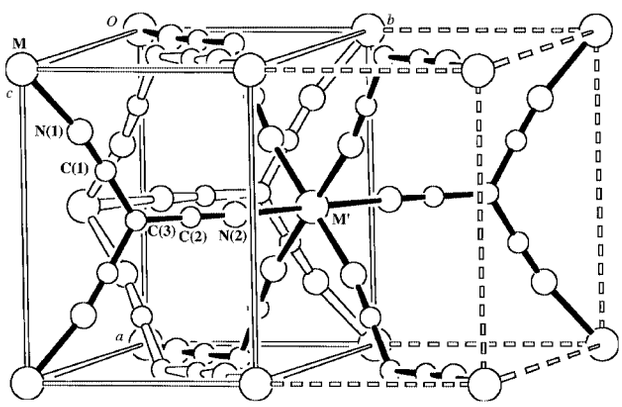

Fig. 2 The unit cell and numbering scheme for $M(tcm)_2$. One framework is continued into an adjoining cell to illustrate the rutile relationship.

M–N type and consequently there is insufficient room for a second rutile network to interpenetrate.

The unit cell and numbering scheme of the $M(tcm)_2$ structures is shown in the left hand half of Fig. 2. One framework (solid black connections) is continued into the unit cell to the right in Fig. 2 in order to reveal its rutile-like connectivity. This diagram shows that although the unit cell dimensions in the *a* and *c* directions are the same as would have been the case if there had been only a single rutile-like network; the presence of the second, identical network leads to a halving of the cell dimension in the *b* direction. The metal atom lies on a site of 2/*m* symmetry, while C2, N2 and C3 all lie on a mirror plane. As can be seen in Fig. 2, one network is generated from the other simply by a translation of one unit cell length along the *b* direction.

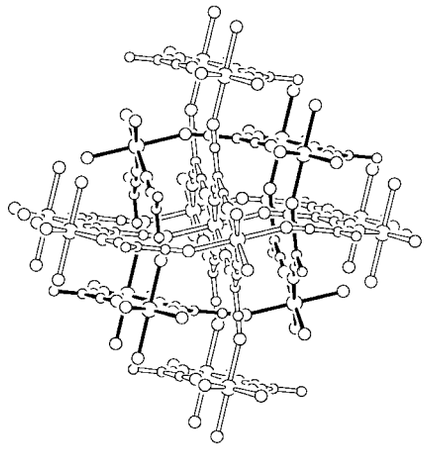

Fig. 3 The two distorted interpenetrating rutile-related networks of $M(tcm)_2$ ($M = Cr^{II}$).

Further insight into the nature of the interpenetration is provided in Fig. 3, which shows a more extended version of the two networks in the particular case of $Cr(tcm)_2$. If one focuses on only the 3-connecting nodes (the central tcm^- C3) and the 6-connecting nodes (M) of the networks, rings of two types can be discerned, six-membered M_3C3_3 rings and four-membered M_2C3_2 rings. The characterising feature of the interpenetration is that each six-membered ring of one framework has a rod belonging to a six-membered ring of the other framework passing through it. The rods protrude through the rings in such a way that the C2 atoms of both frameworks fall almost exactly on a line parallel to *a*. Rods belonging to the four-membered rings, in contrast, are not involved in this way; the ratio between the length of the M–C–C–N rods and their van der Waals radii dictates that the hole at the middle of a four-membered M_2C3_2 ring is too small to allow another rod to pass through it. It is difficult to envisage any other possible mode of structural interpenetration.

An important structural feature revealed in Fig. 3 is the distortion of each framework by the close proximity of the other. The tcm^- ligand remains internally close to planar. The attached metals, however, are forced significantly out of the ligand plane, more so at N1 than at N2; those attached to N1 are displaced from the plane by 0.109, 0.120, 0.128 and 0.126 Å for Cr, Cu, Zn and Hg, respectively and those attached to N2 by 0.794, 0.807, 0.536 and 0.799 Å for the same list of metals. This results in the angle at N2 (*i.e.* the M–N2–C2 angle) being considerably less than 180° (160.9(7)–166.8(2)°). The reason for the distortion appears to stem from the necessity for one framework to minimise unfavourable steric contacts with the other framework. In other words, if the networks were not deformed and if the metals all remained within the plane of their associated tcm, there would be unacceptable steric clashes between the frameworks. These clashes are indicated in Table 3 which also presents the calculated distances of closest approach between the two frameworks in the idealised case where the metals and the tcm^- ligands are artificially made coplanar, and the bond lengths and other angles remain close to those found experimentally (Fig. 4).† It shows that for $Zn(tcm)_2$ (for example) the distances between the frameworks are as low as 2.77 Å, which is sterically unacceptable. Thus the frameworks distort to relieve this steric interaction, such that the smallest inter-framework interatomic distances are now 3.137(4)–3.252(9) Å

† The idealised structure was calculated from the $Zn(tcm)_2$ structure. The coordinates of the tcm^- atoms were adjusted to make the metal and tcm^- atoms coplanar. The coordinates for the model are as follows: Zn 0, 0, 0; C1 0.3403, −0.2704, 0.1352; N1 0.2098, −0.1877, 0.0938; C2 0.5, −0.5559, 0.2779; N2 0.5, −0.7097, 0.3549; C3 0.5, −0.3662, 0.1831. The cell dimensions were adjusted to $a = 7.466$, $b = 5.279$, $c = 10.558$ Å.

Table 2 Selected interatomic distances (Å) and angles (°) for $M(tcm)_2$[a]

	Zn	Cu	Cr	Hg
M–N1	2.120(2)	1.981(1)	2.076(3)	2.317(6)
M–N2^{i}	2.211(2)	2.494(2)	2.475(8)	2.43(1)
N1–M–N1^{ii}	84.4(1)	86.8(1)	86.0(1)	82.9(2)
N1–M–N1^{iii}	95.6(1)	93.2(1)	94.0(1)	97.1(2)
N1–M–N2^{i}	89.1(1)	88.4(1)	88.8(1)	88.2(2)
N1–M–N2^{iv}	90.9(1)	91.6(1)	91.2(1)	91.8(2)
C1–N1–M	170.0(1)	169.7(1)	170.4(3)	169.5(5)
C3–C1–N1	178.5(2)	177.6(1)	177.3(3)	177.9(5)
C1–C3–C1^{v}	117.4(2)	117.0(2)	116.9(4)	110.6(8)
C1–C3–C2	121.2(1)	121.5(1)	121.6(3)	119.7(6)
C3–C2–N2	178.9(3)	179.3(1)	178.3(4)	180.0(7)
C2–N2–M^{vi}	166.8(2)	161.6(1)	162.6(5)	160.9(7)

[a] Symmetry transformations: (i) $\frac{1}{2} - x, 1 + y, \frac{1}{2} - z$; (ii) $x, -y, -z$; (iii) $-x, y, z$; (iv) $\frac{1}{2} - x, y - 1, z - \frac{1}{2}$; (v) $1 - x, y, z$; (vi) $\frac{1}{2} - x, y - 1, \frac{1}{2} - z$.

Table 3 Distances of closest contact (Å) between frameworks for $M(tcm)_2$[a]

Contact	Cr	Cu	Hg	Zn	Zn(ideal)
C3 · · · N1^{i}	3.495(6)	3.504(1)	3.48(1)	3.358(4)	2.98
C3 · · · N1^{ii}	3.495(6)	3.504(1)	3.48(1)	3.358(4)	2.98
C3 · · · C1^{i}	3.598(6)	3.583(1)	3.70(1)	3.531(4)	3.22
C3 · · · C1^{ii}	3.598(6)	3.583(1)	3.70(1)	3.531(4)	3.22
C3 · · · C1^{iii}	3.460(6)	3.442(2)	3.52(1)	3.415(5)	4.05
C3 · · · C1^{iv}	3.460(6)	3.442(2)	3.52(1)	3.415(5)	4.05
C3 · · · C3^{iii}	3.420(8)	3.401(2)	3.49(1)	3.417(6)	4.12
N1 · · · C2^{i}	3.368(6)	3.344(2)	3.35(1)	3.190(4)	2.84
N1 · · · C1^{i}	3.449(5)	3.504(2)	3.343(9)	3.283(3)	2.92
N1 · · · N1^{i}	3.854(5)	3.932(2)	3.680(8)	3.670(4)	3.35
N1 · · · C1^{iv}	3.470(5)	3.459(2)	3.446(8)	3.348(4)	3.87
N1 · · · N1^{iv}	3.552(5)	3.545(2)	3.461(8)	3.384(4)	3.85
N1 · · · N2^{i}	3.659(6)	3.628(2)	3.66(1)	3.479(4)	3.22
C1 · · · C1^{i}	3.252(5)	3.282(2)	3.252(9)	3.137(3)	2.77
C1 · · · C1^{iv}	3.236(5)	3.219(2)	3.255(9)	3.137(3)	3.75
C1 · · · C2^{i}	3.422(5)	3.377(2)	3.531(9)	3.334(4)	3.09
C1 · · · N2^{i}	3.673(5)	3.623(2)	3.803(9)	3.586(4)	3.44

[a] Symmetry transformations: (i) $\frac{1}{2} - x, y, \frac{1}{2} - z$; (ii) $\frac{1}{2} + x, y, \frac{1}{2} - z$; (iii) $1 - x, -1 - y, -z$; (iv) $x, -1 - y, -z$.

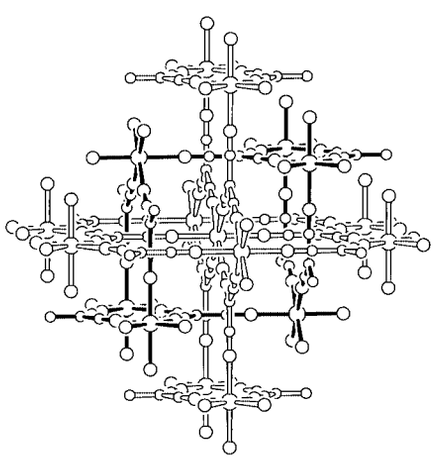

Fig. 4 Two undistorted interpenetrating rutile-related networks of an *idealised* $M(tcm)_2$ model.

(Table 3). This distortion can be clearly seen by comparing Figs. 3 and 4.

The other major deviation from the idealised rutile model in the structure is the bend at N1 (M–N1–C1 169.5(5)–170.4(3)°). This bend is mostly in the plane of the tcm^- ligand, and occurs to relieve the angle strain in the four-membered M_2C3_2 ring. With no bending at N1 and a strictly trigonal geometry at C3 (*i.e.* 120° internal angles), then the N1–M–N1 angle has to be

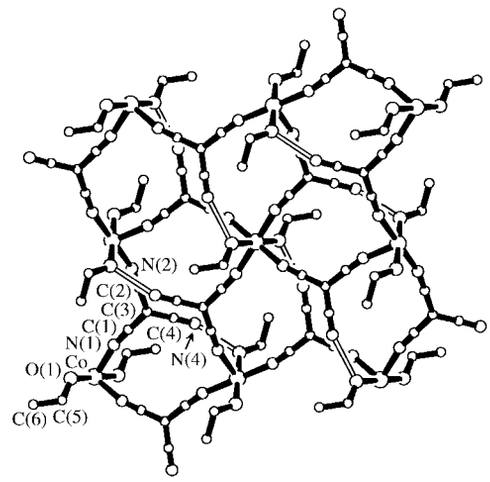

Fig. 5 The structure and atom numbering of $[Co(tcm)_2(EtOH)_2]$. The open bonds represent hydrogen-bonding interactions.

60°. Similarly, if the angles at the metal were 90°, and there were no bending at N1, then the angle at C3 would be unacceptably low (90°). Thus the framework distorts again, mostly at N1, to give acceptable angles at both C3 (C1–C3–C1 110.6(8)–117.4(2)°) and M (N1–M–N1 82.9(2)–86.8(1)°).

Interestingly, the internal geometry of the tcm^- anions remains fairly rigid, despite the severe distortions within the frameworks. The anions are essentially planar and the internal bond lengths and angles are affected by the distortions in only a minor fashion. The structures of both $Cr(tcm)_2$ and $Cu(tcm)_2$ show Jahn–Teller distortions of the metal co-ordination geometry.

The $Cr(tcm)_2$ crystals displayed another notable feature: many months after their synthesis the sky-blue crystals showed no sign of oxidation of the Cr^{II} to Cr^{III}, even though they had been exposed to the atmosphere for all that time. Chromium(II) is normally very sensitive to oxidation; the densely packed and interwoven polymeric structure of $Cr(tcm)_2$ no doubt contributes to its stability by protecting the Cr^{II} from oxidation. The Cr^{II} is not only physically protected from oxidation, but there is also no room in the structure to accommodate the necessary counter ion. Two notable examples of air-stable chromium(II) complexes are the $[Cr_5(CN)_{12}]\cdot 10H_2O$ and $Cs_{0.75}[Cr_{2.125}(CN)_6]\cdot 5H_2O$ compounds, both of which have the Prussian blue structure.[44] The air-stability of these complexes was also attributed to the insoluble polymeric network formed.

$[M(tcm)_2(EtOH)_2]$. The importance of solvents in framework construction is illustrated neatly in the chemistry of cadmium cyanide frameworks.[45] When the same reactions which produced the rutile-related $M(tcm)_2$, $M = Co^{II}$ or Ni^{II}, from water are performed in ethanol, new structures are formed with stoichiometry $M(tcm)_2(EtOH)_2$. The crystals were extremely sensitive to loss of solvent, and the X-ray diffraction was performed on crystals cooled to 150 K. Important bond lengths and angles for $[Co(tcm)_2(EtOH)_2]$ are shown in Table 4; $[Ni(tcm)_2(EtOH)_2]$ was found to have very similar cell parameters and identical systematic absences [$a = 6.826(2)$, $b = 9.651(2)$, $c = 11.685(3)$ Å, $\beta = 97.45(2)°$, $U = 763.3(3)$ Å^3, space group $P2_1/n$ (no. 14)] leading to the conclusion that the two were isomorphous.

The crystal structure of $[Co(tcm)_2(EtOH)_2]$ is composed of infinite two-dimensional sheets each of which possesses an essentially square-grid arrangement of cobalt atoms linked by bridging 2-connecting tcm^- anions (Fig. 5). The tcm^- anions are arranged around the cobalt atoms in a square planar arrangement, and the octahedral geometry of each cobalt is completed by the co-ordination of two ethanol molecules above and below the four tcm^- anions. These ethanol ligands are also

Table 4 Selected interatomic distances (Å) and angles (°) for $[Co(tcm)_2(EtOH)_2]$[a]

Co–N1	2.109(2)	Co–N2^{i}	2.108(3)
Co–O1	2.048(2)	N4 · · · O1^{i}	2.782(4)
N1–Co–O1	90.58(9)	N1–Co–N2^{ii}	91.4(1)
O1–Co–N2^{ii}	88.65(8)	Co–N1–C1	167.6(3)
Co–N2^{i}–C2^{i}	162.2(2)	Co–O1–C5	130.2(2)
N4 · · · O1^{i}–Co^{i}	113.2(1)	N4 · · · O1^{i}–C5^{i}	115.9(2)
C4–N4 · · · O1^{i}	156.8(2)		

[a] Symmetry transformations: (i) $\frac{1}{2} - x, \frac{1}{2} + y, \frac{1}{2} - z$; (ii) $x - \frac{1}{2}, -y - \frac{1}{2}, z - \frac{1}{2}$.

hydrogen bonded (O · · · N4 2.782(4) Å) to the unco-ordinated nitrile of the tcm^- ligands (shown as the open bond in Fig. 5).

In each $Co_4(tcm)_4$ "square" of the sheet two tcm^- ligands on opposing sides direct their hydrogen bonded nitrile towards the opposite side of the square, one hydrogen bonding to an ethanol above the plane, and the other to an ethanol below the plane. These two ethanol ligands are bound to cobalt atoms on diagonally opposite corners of the square. The two remaining tcm^- ligands are directed away from the centre of the square, and into neighbouring squares, such that adjoining squares have the hydrogen bonded connections orientated 90° to each other.

Despite the movement of the tcm^- ligands out of the plane of the cobalt atoms, the geometry around the metal atoms is still close to octahedral (Table 4). The cobalt octahedrons 'tilt' so that the ethanol oxygen atoms can come within hydrogen bonding distance of the unco-ordinated nitrogens (Fig. 5). This tilting, and the subsequent 'buckling' within the sheets, is accommodated by a bend at the co-ordinated tcm^- nitrogens (C1–N1–Co 167.6(3), C2–N2–Co 162.2(2)°), similar to that seen in the rutile structures.

Each cobalt, all of which are equivalent, lies at the origin on a centre of symmetry, so that all tcm^- molecules and all ethanol molecules are also equivalent. Again, the tcm^- remains essentially planar, with all internal bond lengths and angles as expected. The Co–N distances are 2.109(2) and 2.108(3) Å. The Co–O distance (2.048(2) Å) and internal ethanol geometry are also consistent with earlier reports of similar complexes in which ethanol is simultaneously co-ordinated to cobalt and hydrogen bonded.[46] The O1 · · · N4 distance of 2.782(4) Å agrees well with the O · · · N hydrogen bonding distances of 2.733(15) and 2.715(13) Å seen in the $[Sn(CH_3)_3(tcm)(H_2O)]$ structure.[27d]

Magnetic properties

The magnetic susceptibilities of the $M(tcm)_2$ complexes, with M^{II} = Cr, Fe, Co, Ni or Cu, were measured over the temperature range 300–4.2 K in a field of 1 T. Data for $Mn(tcm)_2$ have recently been reported by Miller and co-workers.[42] Experimental data are plotted in Figs. 6–11 and magnetic data are summarised in Table 5. The data are generally indicative of weak antiferromagnetic coupling, except for $Co(tcm)_2$, with no evidence of magnetic long range order occurring when the magnetisations were measured in zero field (ZFCM) and tiny fields (FCM) of 5 Oe. The latter situation contrasts with the abrupt phase transitions noted below *ca.* 20 K in the single net (rutile) dicyanamide analogues $M(N(CN)_2)_2$, M = Mn, Fe, Co or Ni.[38,39] There are unusual magnetic features apparent at low temperatures in some of the present compounds and these are described below. Each system is now described separately, starting from the lowest d^n configuration.

$Cr(tcm)_2$. The compound $Cr(tcm)_2$ has a room temperature moment reduced from the high spin value of 4.87 μ_B *viz.* 4.45 μ_B. It slowly decreases between 300 and 50 K, then more rapidly

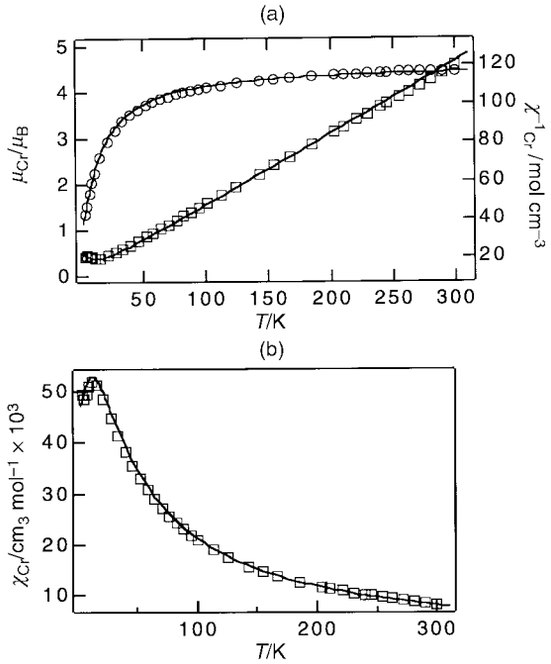

Fig. 6 (a) Plots of μ_{Cr} (○) and $\chi^{-1}{}_{Cr}$ (□) *vs.* temperature for $Cr(tcm)_2$ in a field of 1 T. The solid lines are a guide to the eye. (b) Best-fit to χ_{Cr} data using Heisenberg linear chain model for $S = 2$ modified to include chain–chain interactions. See text for best-fit parameters used to calculate the solid line.

reaching 1.3 μ_B at 4.2 K. The corresponding $\chi^{-1}{}_{Cr}$ plot is linear and Curie–Weiss like above 50 K, with $C = 2.76$ and $\theta = -31.2$ K, but it goes through a broad minimum at 14.5 K (Fig. 6(a)). The χ_{Cr} plot likewise goes through a corresponding maximum indicative of antiferromagnetic coupling, followed by a minimum at 6.2 K [Fig. 6(b)]. The reason for this minimum is not clear, but may be due to traces of monomer impurity being present.

Variation of the applied field values between 0 and 5 T in the temperature region 2–12 K gives straight lines for the *M vs. H* plots at 12 and 7 K, with low values of *M* of *ca.* 0.45 *Nβ* (compared to M_{sat} of $S = 2$ of 4 *Nβ*) again indicative of antiferromagnetic coupling. The 2 K data show a gentle curve but far removed from saturation behaviour. Tests for long range ordering of the ferromagnetic type proved to be negative. The field cooled (5 Oe) and zero field cooled magnetisation plots were identical below 30 K and no hysteresis was noted. Overall, the susceptibility and magnetisation data are similar to those recently reported by Bellitto *et al.*[47] for $Cr_2(O_3P(CH_2)_2PO_3)\cdot 3H_2O$, which is thought to have a 3-D structure made up of phosphonate-bridged layers and PCCP pillars. The present data are different to those of a canted antiferromagnet (weak ferromagnet) which were displayed by $Cr(CH_3PO_3)\cdot H_2O$.[47] The latter shows a field dependence of the maximum in χ_{Cr}, in the range 5–50 K (H = 100 to 1000 Oe) whereas χ_{Cr} for $Cr(tcm)_2$ is independent of field. Interestingly, Bellitto *et al.*[47] proposed that a maximum in χ_{Cr} at 15 K for $Cr_2(O_3P(CH_2)_2PO_3)\cdot 3H_2O$ was possibly due to 3-D antiferromagnetic order. Above 70 K they found good agreement for χ_{Cr} values with the Heisenberg $S = 2$ linear chain model,[48] $J = -4.7$ cm^{-1}. Application of this model to the $Cr(tcm)_2$ data, modified to include a zJ' term for interchain effects,[49] gave a good fit over the whole temperature range for the parameter set $J = -1.6$ cm^{-1}, $zJ' = +0.04$ cm^{-1} and $g = 1.88$ (Fig. 6(b)). The g value is rather low even allowing for spin–orbit effects and may be a result of the limitations of the model used.

$Mn(tcm)_2$. Miller and co-workers[42] found Curie–Weiss behaviour for χ_{Mn} with $\theta = -5.1$ K and μ_{Mn} (300 K) = 5.86 μ_B; μ_{Mn} (2 K) = 3.1 μ_B. Weak antiferromagnetic coupling was

Table 5 Summary of magnetic data for $M(tcm)_2$ complexes

	Cr	Mn[a]	Fe	Co	Ni	Cu
d^n	4	5	6	7	8	9
S (single ion)	2	5/2	2	3/2	1	1/2
$\mu_{eff}/\mu_B \pm 0.02$; 300 K	4.45	5.86	5.18	4.84	3.04	1.89
θ/K ± 0.1	−31.2[b]	−5.1[c]	−25[d]	−5.4[e]	−3.7[f]	[g]
Exchange coupling	A	A (vw)	A (vw-U)	F (vw-U)[h]	A (vw)	A (vw)

A = Antiferromagnetic coupling, F = ferromagnetic coupling, U = uncoupled, vw = very weak. [a] Ref. 42. [b] 50–300 K region. [c] 2–300 K region (ref. 42). [d] 170–300 K region. [e] 100–300 K region. [f] 30–300 K region. [g] Gently curved χ^{-1}_{Cu} *vs.* T plot with linear portion between 4 and 100 K, $\theta = -1.7$ K. [h] Very weak ferromagnetic coupling below 10 K.

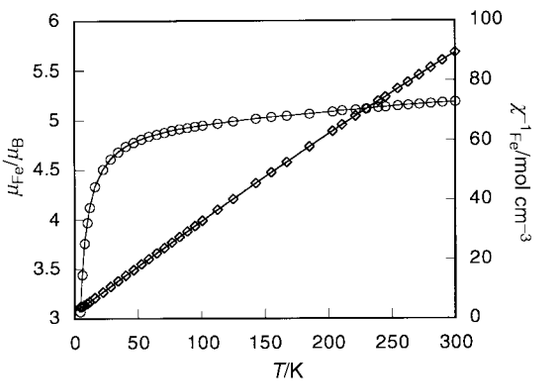

Fig. 7 Plots of μ_{Fe} (○) and χ^{-1}_{Fe} (□) *vs.* temperature for $Fe(tcm)_2$ in a field of 1 T. The solid lines are a guide to the eye.

proposed arising, possibly, from a combination of internetwork dipolar coupling and intranetwork super-exchange interactions, *via* $C(CN)_3^-$ bridges.

$Fe(tcm)_2$. The room temperature μ_{eff} value of 5.18 μ_B is indicative of a high spin octahedral d^6 system with single ion $^5T_{2g}$ ground states. The moment decreases gradually between 300 and 50 K, then rapidly, reaching 3.1 μ_B at 4.2 K. The χ^{-1}_{Fe} plot is broadly Curie–Weiss like (Fig. 7) although with gradual curvature to a lower θ at low temperature. Between 300 and 170 K the linear portion has $\theta = -25$ K. While generally indicative of uncoupled $^5T_{2g}$ ground states, the magnetic data are influenced by a combination of orbital degeneracy, low-symmetry, ligand-field splitting, zero field splitting, z.f.s. (at low temperatures) and antiferromagnetic coupling.[50] There is no indication in very low fields of a magnetic phase transition of the type noted for the spin canted antiferromagnet $Fe(N(CN)_2)_2$, at $T_N = 19$ K.[38e,39a]

$Co(tcm)_2$. Curie–Weiss behaviour is followed when χ_{Co} values are measured in a field of 1 T, with $\theta = -5.4$ K. The μ_{Co} values remain approximately constant at 4.84 μ_B between 300 and 100 K, then decrease more rapidly to reach a minimum value of 4.2 μ_B at 10 K, followed by an increase to 4.24 μ_B at 4.2 K [Fig. 8(a)]. The latter feature is most unusual for high spin octahedral cobalt(II) compounds which have single-ion $^4T_{1g}$ parent ground states,[51] capable of being affected by the same perturbations described above for $Fe(tcm)_2$. It can be seen in Fig. 8(b) that the μ_{Co} values are being sensitively affected by variations in the applied field at temperatures between *ca.* 20 and 2 K. In a 1 T field the μ_{Co} values actually go through a 'minimax' behaviour, finally decreasing rapidly to 3.95 μ_B at 2 K. In fields of 5000, 1000 and 100 Oe the μ_{Co} values show only the broad minimum between 20 and 10 K, followed by a rapid increase below 10 K. The value of μ_{Co} at 2 K does not, however, increase as strongly to very high values as would be the case if long-range ferromagnetic order were occurring in applied fields such as 100 Oe, but rather begins to attenuate. Tests for long range order in very small fields of 5 Oe proved negative. This contrasts with the ferromagnetic order found in $Co(dca)_2$ with a T_c value of 9 K.[38a]

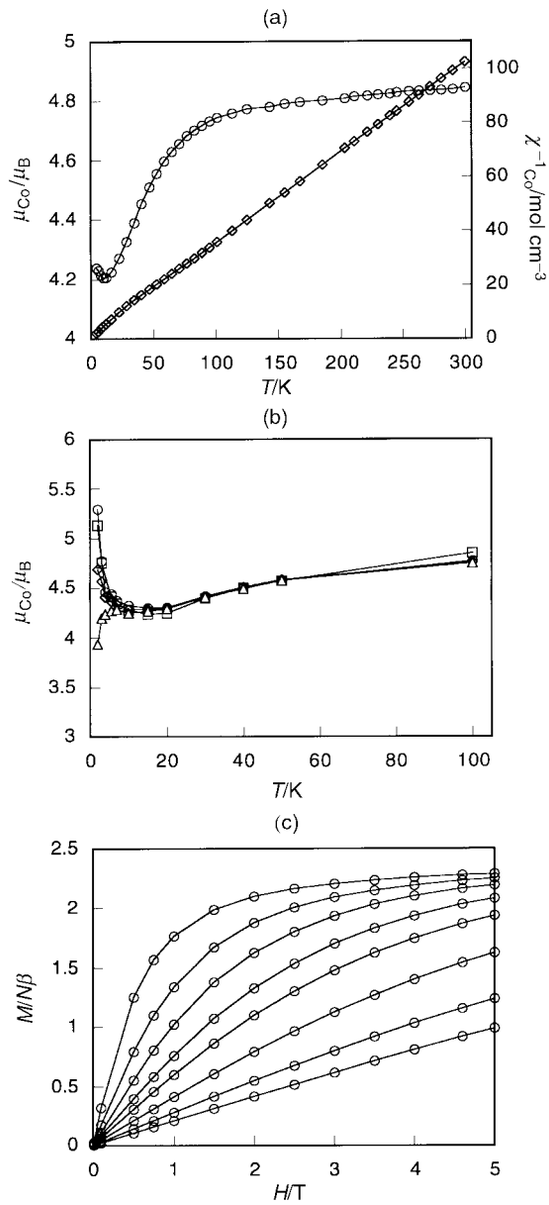

Fig. 8 (a) Plots of μ_{Co} (○) and χ^{-1}_{Co} (□) *vs.* temperature for $Co(tcm)_2$ in a field of 1 T. (b) μ_{Co} values observed in fields of 10 000 (△), 5000 (◇), 1000 (□) and 100 (○) Oe, over the range 2–100 K. (*c*) High field magnetisation isotherms obtained at temperatures of 2 (top), 3, 4, 5.5, 7, 10, 15 and 20 K (bottom). The solid lines are a guide to the eye.

High field magnetisation isotherms, shown in Fig. 8(c) for $Co(tcm)_2$, indicate that saturation occurs at 2 K with an M_{sat} value of 2.3 $N\beta$, which is less than the $S = 3/2$ value of 3 $N\beta$. Possible reasons for this low M_{sat} value include ground state zero field splitting, ligand field effects, or superimposed antiferromagnetic coupling. The unusual field dependent μ_{Co} behaviour at low and decreasing temperatures is most likely

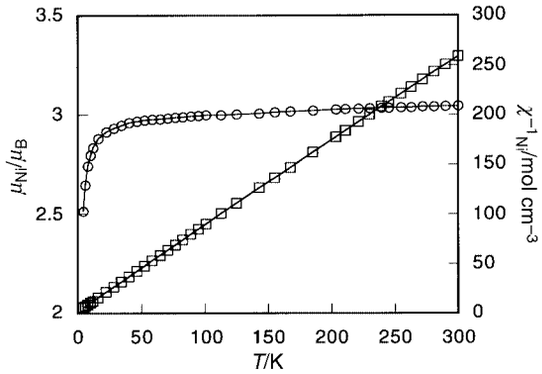

Fig. 9 Plots of μ_{Ni} (○) and $\chi^{-1}{}_{Ni}$ (□) *vs.* temperature for Ni(tcm)$_2$ in a field of 1 T. The solid lines are a guide to the eye.

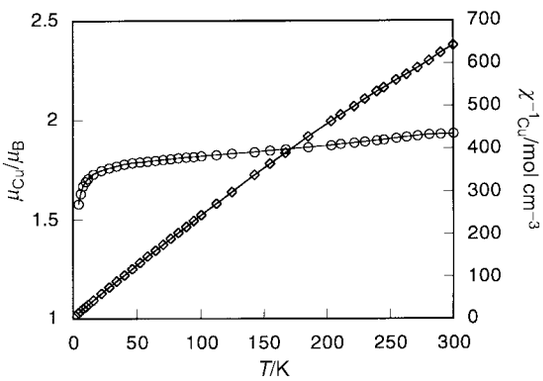

Fig. 10 Plots of μ_{Cu} (○) and $\chi^{-1}{}_{Cu}$ (□) *vs.* temperature for Cu(tcm)$_2$ in a field of 1 T. The solid lines are a guide to the eye.

indicative of the thermal depopulation of closely spaced Zeeman levels. The nature of the energy levels is likely to be very complex, resulting from single-ion ligand field and z.f.s. effects, as well as possible weak ferromagnetic coupling, evident at very low temperatures. We have recently observed similar field dependent behaviour at low temperatures, and similar high field *M vs. H* isotherms for the sheet-like dicyanamide polymer [Ph_4As][Co(dca)$_3$], which contains high spin octahedral cobalt(II) centres bridged by bidentate dca$^-$ ligands.[52] This suggests that it is not due to a ferromagnetically coupled or ordered impurity. We are not aware of such behaviour in any other cobalt(II) system. To test out the possible origin of the field dependent μ_{Co} values, calculation of z.f.s. for $S = 3/2$, appropriately scaled by g to present μ_{Co} values, gave no increase in μ_{Co} irrespective of the sign of z.f.s. Use of a simple trimer $S = 3/2$ model and $J = +0.1$ cm^{-1} does yield μ_{Co} values at 2 K which are higher, and increasing, for fields less than 7000 Oe, and lower for fields greater than 7000 Oe. Thus it seems highly likely that very weak intranetwork ferromagnetic coupling is occurring in Co(tcm)$_2$ (and in [Ph_4As][Co(dca)$_3$]).[52]

Ni(tcm)$_2$. The μ_{Ni} and $\chi^{-1}{}_{Ni}$ *vs.* temperature data (Fig. 9) are as expected for an essentially uncoupled octahedral Ni^{II} system. A small Weiss constant of −3.7 K and rapid decrease in μ_{Ni} occurring below 30 K are indicative of very weak antiferromagnetic coupling combined with z.f.s. of the single ion $^3A_{2g}$ states.

Cu(tcm)$_2$. The magnetic data shown in Fig. 10 are again indicative of very weak antiferromagnetic coupling. The $\chi^{-1}{}_{Cu}$ *vs. T* plot shows a gradual shallow curvature. Since Cu(tcm)$_2$(Hpz)$_2$ (Hpz = pyrazole) chain complexes generally show linear $\chi^{-1}{}_{Cu}$ *vs. T* behaviour and very weak coupling,[27a–c] it is possible that the deviation from linearity and concomitant gradual decrease in μ_{Cu} arise from interchain effects.

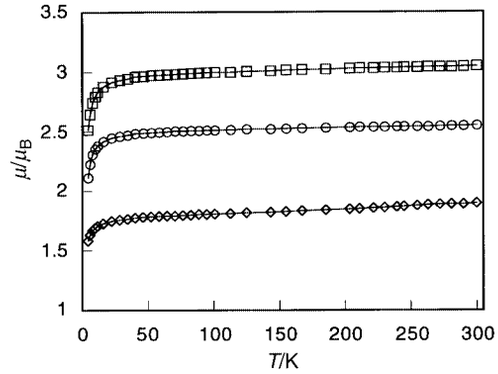

Fig. 11 Plots of μ *vs.* temperature for Ni(tcm)$_2$ (□), Ni/Cu(tcm)$_2$ (50:50) (○) and Cu(tcm)$_2$ (◇) in a field of 1 T. The solid lines are a guide to the eye.

Solid solutions of M/M′(tcm)$_2$. Reaction of 50:50 mixtures of M(NO$_3$)$_2$ and M′(NO$_3$)$_2$ with K(tcm) leads to the formation of crystalline products M/M′(tcm)$_2$ which are crystallographically isomorphous with the M(tcm)$_2$ series (at least for Co/Cu and Mn/Co, whose cell parameters, determined from single crystals, are shown in Table 1). Full crystallographic analysis of the mixed metal Co/Cu(tcm)$_2$ species indicated only one crystallographically independent metal position, implying random occupancy of M sites by M′. The desirable situations of having either separate M(tcm)$_2$ and M′(tcm)$_2$ nets, or having regular bimetallic chains ... M(tcm)$_2$M′(tcm)$_2$ ... within each net, is not realised. In retrospect this was not surprising. The systems Co/Ni(tcm)$_2$, Co/Cu(tcm)$_2$ and Ni/Cu(tcm)$_2$ were investigated and the observed magnetic moments at 300 K were very close in value to those calculated for 50:50 M:M′ stoichiometry, *viz.* Co/Ni(tcm)$_2$ $\mu_{obs} = 4.02$ μ_B (calc. 4.04 μ_B), Co/Cu(tcm)$_2$ $\mu_{obs} = 3.73$ μ_B (3.67 μ_B) and Ni/Cu(tcm)$_2$ $\mu_{obs} = 2.55$ μ_B (2.53 μ_B). The 4–300 K μ vs. temperature plots follow the shapes anticipated for 50:50 mixtures, a typical example being given for Ni/Cu(tcm)$_2$ in Fig. 11. Those containing Co(tcm)$_2$ again display the unusual low temperature behaviour of the kinds shown in Fig. 8(a) and 8(b).

Conclusion

Reaction of octahedral metal ions with trigonal tcm$^-$ anions results in the formation of two interpenetrating rutile-like M(tcm)$_2$ networks. The geometric requirements of the metal atoms and ligands, and steric interactions between the two interpenetrating networks, result in distortions within the frameworks. When the reaction is performed in ethanol sheet-like M(tcm)$_2$(EtOH)$_2$ structures are formed, illustrating that variation of the solvent medium can result in formation of entirely new products.

The weak antiferromagnetic or ferromagnetic coupling observed in the M(tcm)$_2$ interpenetrating rutile-like network systems is rather similar to that noted by Hvastijova and coworkers[27a–c] for chain complexes of type M(tcm)$_2$L$_2$, where M^{II} = Co, Ni or Cu; L = substituted pyridines, pyrazole, *etc.* Disappointingly, there is no evidence for long range magnetic order being induced by interpenetration. This situation contrasts with that found in the related M(dca)$_2$ single net system, in which a fascinating variety of magnet types was noted.[38,39] Presumably the differences in geometry across the tcm$^-$ and dca$^-$ bridges, as well as differences in super-exchange interactions, favour long range effects in the M(dca)$_2$ compounds, except for Cu(dca)$_2$ which behaves rather like its Cu(tcm)$_2$ analogue. The curvature in the Curie–Weiss plot for the latter complex is perhaps indicative of weak internetwork effects. Attempts to induce magnetic order by making 50:50 solid solutions of M/M′(tcm)$_2$ simply led to magnetic behaviour

intermediate between that of each parent phase. We are investigating other interpenetrating network species based on $M(dca)_2$ precursors in attempts to assess the structural and electronic features which lead to long range order.[33]

Experimental

Preparations

The compound K(tcm) was prepared according to the literature.[28] All other chemicals were used as supplied.

[Me_4N][tcm]. Solutions of K(tcm) (20 g, 0.155 mol) in hot water (50 cm^3) and Me_4NBr (24 g, 0.156 mol) in hot water (50 cm^3) were mixed, and the total volume was reduced to 75 cm^3 by boiling. The solution was allowed to cool, giving colourless crystalline rods of [Me_4N][tcm] (2.16 g, 0.132 mol, 85% yield).

M(tcm)$_2$. The homometallic $M(tcm)_2$ complexes (except M = Cr or Hg) were prepared according to the methods described in the literature.[28,29] Crystals of each were grown as detailed below.

Cu(tcm)$_2$. A hot solution of $Cu(NO_3)_2 \cdot 3H_2O$ (190 mg, 0.786 mmol) in water (8 cm^3) was added to a hot solution of K(tcm) (200 mg, 1.55 mmol) in water (6 cm^3), then allowed to cool. Dark brown crystals separated some time after the solution had reached room temperature. These were then collected and air dried (131 mg, 0.538 mmol, 69% yield).

Zn(tcm)$_2$. A hot solution of $Zn(NO_3)_2 \cdot 3H_2O$ (230 mg, 0.773 mmol) in water (1 cm^3) was added to a hot solution of K(tcm) (200 mg, 1.55 mmol) in water (1 cm^3) then allowed to cool. Large clear, colourless crystals separated some time after the solution had reached room temperature. These were then collected and air dried (46 mg, 0.187 mmol, 24% yield).

Cd(tcm)$_2$. A hot solution of $Cd(NO_3)_2 \cdot 4H_2O$ (240 mg, 0.778 mmol) in water (8 cm^3) was added to a hot solution of K(tcm) (200 mg, 1.55 mmol) in water (6 cm^3) then allowed to cool. Large clear, colourless crystals separated some time after the solution had reached room temperature. These were then collected and air dried (134 mg, 0.458 mmol, 59% yield).

Mn(tcm)$_2$. A hot solution of $MnCl_2 \cdot 4H_2O$ (153 mg, 0.778 mmol) in water (2 cm^3) was added to a hot solution of K(tcm) (200 mg, 1.55 mmol) in water (1 cm^3) then allowed to cool. Large clear, colourless crystals separated some time after the solution had reached room temperature. These were then collected and air dried (100 mg, 0.425 mmol, 55% yield).

Co(tcm)$_2$. A hot solution of $Co(NO_3)_2 \cdot 6H_2O$ (225 mg, 0.773 mmol) in water (8 cm^3) was added to a hot solution of K(tcm) (200 mg, 1.55 mmol) in water (6 cm^3) then heated in a water-bath at 75 °C for 24 h. The resulting orange pentagonal bipyramidal crystals were collected and air dried (68 mg, 0.284 mmol, 36% yield).

Ni(tcm)$_2$. A hot solution of $Ni(NO_3)_2 \cdot 6H_2O$ (225 mg, 0.773 mmol) in water (8 cm^3) was added to a hot solution of K(tcm) (200 mg, 1.55 mmol) in water (6 cm^3) then heated in a water-bath at 85 °C for 12 d. The resulting small blue pentagonal bipyramidal crystals were collected and air dried (140 mg, 0.586 mmol, 76% yield).

Cr(tcm)$_2$. Chromium metal (20 mg, 0.38 mmol) was dissolved under nitrogen in 10 cm^3 98% H_2SO_4 and 30 cm^3 of water. The compound [Me_4N][tcm] (126 mg, 0.77 mmol) was added, and sky blue crystals of $Cr(tcm)_2$ started forming soon afterwards and were filtered off after 24 h (7.5 mg, 0.032 mmol, 8% yield).

Hg(tcm)$_2$. Solutions of $Hg(ClO_4)_2 \cdot 3H_2O$ (25 mg, 0.055 mmol) in 10 cm^3 of acetonitrile and [Me_4N][tcm] (18 mg, 0.11 mmol) in 10 cm^3 of acetonitrile were combined to give colourless crystalline needles of $Hg(tcm)_2$ (11.3 mg, 0.030 mmol, 55% yield).

Co/Cu(tcm)$_2$. A hot solution of $Co(NO_3)_2 \cdot 6H_2O$ (44 mg, 0.150 mmol) and $Cu(NO_3)_2 \cdot 3H_2O$ (36 mg, 0.150 mmol) in water (4 cm^3) was added to a hot solution of K(tcm) (79 mg, 0.61 mmol) in water (4 cm^3). Dark orange pentagonal bipyramidal crystals were collected after several days (42 mg, 0.174 mmol, 58% yield). Examination of the product under the microscope showed it to be homogeneous, with no sign of $Cu(tcm)_2$ crystals, and the crystals were much darker in appearance compared to the $Co(tcm)_2$ crystals. The samples of Co/Ni$(tcm)_2$, Ni/Cu$(tcm)_2$ and Mn/Co$(tcm)_2$ were prepared similarly.

[Co(tcm)$_2$(EtOH)$_2$]. A careful layering of, in ascending order, a solution of $Co(NO_3)_2 \cdot 6H_2O$ (50 mg, 0.17 mmol) in 5 cm^3 of ethanol, a 5 cm^3 'buffer' of neat ethanol, and then [Me_4N][tcm] (56.3 mg, 0.34 mmol) in 5 cm^3 of ethanol produced orange crystals of $[Co(tcm)_2(EtOH)_2]$ (12.1 mg, 0.037 mmol, 22% yield) after nine days. They were sensitive to loss of solvent.

[Ni(tcm)$_2$(EtOH)$_2$]. A careful layering of, in ascending order, a solution of $Ni(NO_3)_2 \cdot 6H_2O$ (46 mg, 0.16 mmol) in 5 cm^3 of ethanol, a 5 cm^3 'buffer' of neat ethanol, and then [Me_4N][tcm] (51.9 mg, 0.32 mmol) in 5 cm^3 of ethanol produced blue crystals of $[Ni(tcm)_2(EtOH)_2]$ after five months. They were sensitive to loss of solvent. $\rho_c = 1.44$ g cm^{-3}, $\rho_e = 1.42(1)$ g cm^{-3}.

Crystallography

M(tcm)$_2$. The cobalt and nickel (and Co/Cu) compounds gave only pentagonal bipyramidal crystals, which were found to be five separate intergrown crystals. For these compounds the crystallography was performed on one of the five wedge-shaped crystals obtained by carefully applying pressure to the pentagonal bipyramid between two glass slides. Separate wedge-shaped crystals and pentagonal bipyramidal crystals with 'missing' wedges were also seen in a number of other compounds.

The structures were solved from the Patterson functions (SHELXS 86).[53] Refinements were achieved using the SHELX 76 system.[54] Anisotropic thermal parameters were applied to all atoms.

The structure of Co/Cu$(tcm)_2$ was solved using data collected similarly on an Enraf-Nonius CAD-4MachS diffractometer using Cu-Kα radiation ($\lambda = 1.5418$ Å). Data were treated similarly, and the structure solved using the SHELX 97 package,[55] with refinements against F^2. It was refined with 50 : 50 occupation of the single crystallographically unique metal site by Co and Cu. Further details are shown in Table 6.

Crystals of $M(tcm)_2$, M = Mn, Co, Ni or Cd, were treated as above and found to have similar cell parameters and identical systematic absences to those of the fully characterised $M(tcm)_2$ structures. Consequently full data sets were not collected. The mixture Mn/Co$(tcm)_2$ was also found to have similar cell parameters.

[M(tcm)$_2$(EtOH)$_2$]. Crystal data and details of the structure determination for $[Co(tcm)_2(EtOH)_2]$ are presented in Table 6. All details of data collection and structure solution are the same as for $M(tcm)_2$, except where specifically stated.

No correction for absorption effects was made. The structure was solved from the Patterson functions. The aliphatic hydrogens were found in subsequent difference maps, and all were assigned to calculated positions (C–H 1.08 Å), and refined with a common isotropic thermal parameter. The alcohol hydrogen was also found and was allowed to refine freely. Anisotropic thermal parameters were applied to all non-hydrogen atoms.

A blue rod of $[Ni(tcm)_2(EtOH)_2]$, sensitive to solvent loss, was treated similarly and found to have similar cell parameters and identical systematic absences to those of the cobalt and thus a full data set was not collected.

CCDC reference number 186/1564.

Table 6 Crystal data together with details of data collection and structure refinement for $M(tcm)_2$ (M = Cr, Cu, Zn, Hg or Co/Cu) and $[Co(tcm)_2(EtOH)_2]$

	$Cr(tcm)_2$	$Cu(tcm)_2$	$Zn(tcm)_2$	$Hg(tcm)_2$	$Co/Cu(tcm)_2$	$[Co(tcm)_2(EtOH)_2]$
Colour of crystal	Sky blue	Dark brown	Colourless	Colourless	Dark orange	Orange
Formula	C_8N_6Cr	C_8N_6Cu	C_8N_6Zn	C_8N_6Hg	$C_8N_6Co_{0.5}Cu_{0.5}$	$C_{12}H_{12}CoN_6O_2$
Formula weight	232.14	243.68	245.51	380.73	241.38	331.23
Crystal system	Orthorhombic	Orthorhombic	Orthorhombic	Orthorhombic	Orthorhombic	Monoclinic
Space group	*Pmna* (no. 53)	*Pmna* (no. 53)	*Pmna* (no. 53)	*Pmna* (no. 53)	*Pmna* (no. 53)	$P2_1/n$ (no. 14)
a/Å	7.330(1)	7.168(1)	7.466(2)	7.833(2)	7.363(1)	6.819(2)
b/Å	5.545(1)	5.4680(6)	5.3171(5)	5.535(1)	5.302(1)	9.677(3)
c/Å	10.743(2)	10.764(1)	10.482(2)	10.759(2)	10.492(2)	11.805(4)
β/°						97.81(3)
U/Å^3	431.9(2)	421.9(1)	416.1(2)	466.4(2)	409.6(1)	717.9(5)
Z	2	2	2	2	2	2
T/K	295(1)	295(1)	295(1)	295(1)	295(1)	150(1)
μ/cm^{-1}	12.31	25.3	29.6	164.41	98.60	10.93
Data measured	1117	1635	1365	1682	1216	2718
Unique data	679	1181	971	1086	460	2042
R_{int}	0.0135	0.010	0.034	0.0268	0.1131	0.0204
Observed data $[I \geq 3\sigma(I)]$	406	982	738	652	410 (2σ)	1019
Final R	0.0419	0.030	0.030	0.0284	R (obs. data) 0.0480	0.0368
Final R'	0.0374	0.036	0.033	0.0265	$wR2$ (all data) 0.1291	0.0279

Magnetic measurements

A Quantum Design MPMS5 SQUID magnetometer was employed for susceptibility and detailed magnetisation measurements, as described previously.[56] Samples were finely ground and contained in gelatine capsules held at the centre of a drinking straw attached to the sample rod. Measurements of $Cr(tcm)_2$ were repeated at an interval of one year and identical data were obtained indicating that no oxidation had occurred.

Acknowledgements

This work was supported by grants from the Australian Research Council (ARC Large Grants) to K. S. M. and R. R. The receipt of an ARC Postdoctoral Fellowship (by S. R. B.) is gratefully acknowledged.

References

1 (*a*) B. F. Hoskins and R. Robson, *J. Am. Chem. Soc.*, 1990, **112**, 1546; (*b*) R. Robson, B. F. Abrahams, S. R. Batten, R. W. Gable, B. F. Hoskins and J. Liu, *ACS Symp. Ser.*, 1992, **499**, 256; (*c*) R. Robson, *Comprehensive Supramolecular Chemistry*, eds. J. L. Atwood, J. E. D. Davies, D. D. MacNicol, F. Vogtle and J.-M. Lehn, Pergamon, Oxford, 1997, vol. 6, p. 733; (*d*) S. R. Batten and R. Robson, *Angew. Chem., Int. Ed.*, 1998, **37**, 1460.

2 K. A. Hirsch, S. C. Wilson and J. S. Moore, *Chem. Eur. J.*, 1997, **3**, 765; O. M. Yaghi, C. E. Davis, G. Li and H. Li, *J. Am. Chem. Soc.*, 1997, **119**, 2861; M. J. Zaworotko, *Chem. Soc. Rev.*, 1994, **23**, 284; L. Carlucci. G. Ciani, D. M. Proserpio and A. Sironi, *J. Chem. Soc., Chem. Commun.*, 1994, 2755; D. M. L. Goodgame, S. Menzer, A. M. Smith and D. J. Williams, *J. Chem. Soc., Dalton Trans.*, 1997, 3213; M. A. Withersby, A. J. Blake, N. R. Champness, P. Hubbertsey, W.-S. Li and M. Schroder, *Angew. Chem., Int. Ed. Engl.*, 1997, **36**, 2327; M. Munakata, L. P. Wu, T. Kuroda-Sowa, M. Maekawa, K. Moriwaki and S. Kitagawa, *Inorg. Chem.*, 1997, **36**, 5416.

3 G. B. Gardner, D. Venkataraman, J. S. Moore and S. Lee, *Nature* (*London*), 1995, **374**, 792; D. Venkataraman, G. B. Gardner, S. Lee and J. S. Moore, *J. Am. Chem. Soc.*, 1995, **117**, 11600; D. Venkataraman, S. Lee, J. S. Moore, P. Zhang, K. A. Hirsch, G. B. Gardner, A. C. Covey and C. L. Prentice, *Chem. Mater.*, 1996, **8**, 2030; G. B. Gardner, Y.-H. Kiang, S. Lee, A. Asgaonkar and D. Venkataraman, *J. Am. Chem. Soc.*, 1996, **118**, 6946.

4 O. M. Yaghi, H. Li and T. L. Groy, *J. Am. Chem. Soc.*, 1996, **118**, 9096; O. M. Yaghi, G. Li and H. Li, *Nature* (*London*), 1995, **378**, 703; O. M. Yaghi, R. Jernigan, H. Li, C. E. Davis and T. L. Groy, *J. Chem. Soc., Dalton Trans.*, 1997, 2383; C. Janiak and H. Hemling, *J. Chem. Soc., Dalton Trans.*, 1994, 2947; M. Hill, M. F. Mahon and K. C. Molloy, *J. Chem. Soc., Dalton Trans.*, 1996, 1857; A. Michaelides, S. Skoulika, V. Kiritsis, C. Raptopoulou and A. Terzis, *J. Chem. Res.* (*S*), 1997, 204; L. Carlucci, G. Ciani, D. W. v. Gudenberg, D. M. Proserpio and A. Sironi, *Chem. Commun.*, 1997, 631; L. Carlucci, G. Ciani, D. M. Proserpio and A. Sironi, *Inorg. Chem.*, 1997, **36**, 1736; *J. Am. Chem. Soc.*, 1995, **117**, 12861; H. Iwamura, K. Inoue and N. Koga, *New J. Chem.*, 1998, **22**, 201; C. J. Kepert and M. J. Rosseinsky, *Chem. Commun.*, 1998, 31.

5 (*a*) S. R. Batten, Ph.D. Thesis, University of Melbourne, 1995; (*b*) B. F. Abrahams, S. R. Batten, H. Hamit, B. F. Hoskins and R. Robson, *Chem. Commun.*, 1996, 1313; (*c*) S. R. Batten, B. F. Hoskins and R. Robson, *J. Am. Chem. Soc.*, 1995, **117**, 5385; (*d*) S. R. Batten, B. F. Hoskins and R. Robson, *Angew. Chem., Int. Ed. Engl.*, 1995, **34**, 820; (*e*) B. F. Abrahams, S. R. Batten, H. Hamit, B. F. Hoskins and R. Robson, *Angew. Chem., Int. Ed. Engl.*, 1996, **35**, 1690; (*f*) B. F. Abrahams, S. R. Batten, M. J. Grannas, H. Hamit, B. F. Hoskins and R. Robson, *Angew. Chem., Int. Ed.*, 1999, **38**, 1475.

6 B. F. Abrahams, P. A. Jackson and R. Robson, *Angew. Chem., Int. Ed.*, 1998, **37**, 2656.

7 F.-Q. Liu and T. D. Tilley, *Inorg. Chem.*, 1997, **36**, 5090.

8 B. F. Abrahams, B. F. Hoskins and R. Robson, *J. Am. Chem. Soc.*, 1991, **113**, 3606; B. F. Abrahams, B. F. Hoskins, D. M. Michail and R. Robson, *Nature* (*London*), 1994, **369**, 727.

9 H. Schmidtman, *Ber. Bunsenges. Phys. Chem.*, 1896, **29**, 1172; A. Hantzsch and G. Oswald, *Ber. Bunsenges. Phys. Chem.*, 1899, **32**, 641; L. Birkenbach and K. Huttner, *Ber. Bunsenges. Phys. Chem.*, 1929, **62B**, 153, 2065; L. Birkenbach and K. Kellermann, *Ber. Bunsenges. Phys. Chem.*, 1925, **58**, 786.

10 R. H. Boyd, *J. Am. Chem. Soc.*, 1961, **83**, 4288; *J. Phys. Chem.*, 1963, **67**, 737; R. G. Pearson and R. L. Dillon, *J. Am. Chem. Soc.*, 1953, **75**, 2439; S. Trofimenko, *J. Org. Chem.*, 1963, **28**, 217.

11 E. Cox and A. Fontaine, *Bull. Soc. Chim. Fr.*, 1954, 948.

12 W. J. Middleton, E. L. Little, D. D. Coffman and V. A. Engelhardt, *J. Am. Chem. Soc.*, 1958, **80**, 2795.

13 R. H. Boyd, *J. Phys. Chem.*, 1963, **67**, 737 and refs. therein.

14 H. Kohler, in *Chemistry of Pseudohalides*, eds. A. M. Golub, H. Kohler and V. V. Skopenko, Elsevier, Amsterdam, 1987.

15 C. Bugg, R. Desiderato and R. L. Sass, *J. Am. Chem. Soc.*, 1964, **86**, 3157; R. Desiderato and R. L. Sass, *Acta Crystallogr.*, 1965, **18**, 1.

16 P. Andersen, B. Klewe and E. Thom, *Acta Chem. Scand.*, 1967, **21**, 1530.

17 P. Andersen and B. Klewe, *Nature* (*London*), 1963, **200**, 464; J. R. Witt and D. Britton, *Acta Crystallogr., Sect. B*, 1971, **27**, 1835.

18 J.-C. Wang, L.-Y. Chou and W.-Y. Hsien, *Acta Crystallogr., Sect. C*, 1994, **50**, 879; V. V. Skopenko and A. A. Kapshuk, *Koord. Khim.*, 1985, **11**, 1202; M. A. Beno, H. H. Wang, L. Soderholm, K. D. Carlson, L. N. Hall, L. Nunez, H. Rummens, B. Anderson, J. A. Schlueter, J. M. Williams, M.-H. Whangbo and M. Evain, *Inorg. Chem.*, 1989, **28**, 150; D. A. Dixon, J. C. Calabrese and J. S. Miller, *J. Am. Chem. Soc.*, 1986, **108**, 2582; T. V. Baukova, D. N. Kravtsov, L. G. Kuzmina, N. V. Dvortsova, M. A. Poray-Koshits and E. G. Perevalova, *J. Organomet. Chem.*, 1989, **372**, 465; I. Potocnak, M. Dunaj-Jurco, D. Miklos and L. Jager, *Acta Crystallogr., Sect. C*, 1998, **54**, 313; 1996, **52**, 48.

19 J.-C. Wang and Y. Wang, *Acta Crystallogr.*, *Sect. C*, 1993, **49**, 131; D. A. Summerville, I. A. Cohen, K. Hatano and W. R. Scheidt, *Inorg. Chem.*, 1978, **17**, 2906; T. J. Johnson, M. R. Bond and R. D. Willett, *Acta Crystallogr.*, *Sect. C*, 1988, **44**, 1890; S. L. Schiavo, G. Bruno, P. Zanello, F. Laschi and P. Piraino, *Inorg. Chem.*, 1997, **36**, 1004; I. Potocnak, M. Dunaj-Jurco, D. Miklos and L. Jager, *Acta Crystallogr.*, *Sect. C*, 1997, **53**, 1215.
20 J. C. Wang, *Diss. Abstr. B*, 1988, **49**, 1697; J. C. Wang, L. J. Shih, Y.-J. Chen, Y. Wang, F. R. Fronczek and S. F. Watkins, *Acta Crystallogr.*, *Sect. B*, 1993, **49**, 680; M. E. Witt, *Diss. Abstr. B*, 1974, **35**, 723.
21 See also H. Yasuba, T. Imai, K. Okamoto, S. Kusabayashi and H. Mikawa, *Bull. Chem. Soc. Jpn.*, 1970, **43**, 3101; T. Tamamura, M. Yokoyama, S. Kusabayashi and H. Mikawa, *Bull. Chem. Soc. Jpn.*, 1974, **47**, 442; T. Tamamura, H. Yasuba, K. Okamoto, T. Imai, S. Kusabayashi and H. Mikawa, *Bull. Chem. Soc. Jpn.*, 1974, **47**, 448; E. J. Gabe, J. R. Morton, K. F. Preston, P. J. Krusic, D. A. Dixon, E. Wasserman and J. S. Miller, *J. Phys. Chem.*, 1989, **93**, 5337; L. Jager, M. Kretschmann and H. Kohler, *Z. Anorg. Allg. Chem.*, 1992, **611**, 68; A. Gunasekaran and J. H. Boyer, *Heteroatom. Chem.*, 1992, **3**, 611; Y. A. Pentin, D. I. Makhonkov, L. Y. Dyachkova, I. I. Baburina and N. S. Zefirov, *Zh. Obshch. Khim.*, 1978, **48**, 1840; H. Kohler and B. Seifert, *Z. Anorg. Allg. Chem.*, 1966, **344**, 63.
22 J. Konnert and D. Britton, *Inorg. Chem.*, 1966, **5**, 1193.
23 S. R. Batten, B. F. Hoskins and R. Robson, *New J. Chem.*, 1998, **22**, 173.
24 S. R. Batten, B. F. Hoskins and R. Robson, *Angew. Chem.*, *Int. Ed. Engl.*, 1997, **36**, 636.
25 S. R. Batten, B. F. Hoskins and R. Robson, *Inorg. Chem.*, 1998, **37**, 3432.
26 S. R. Batten, B. F. Hoskins and R. Robson, *Chem. Eur. J.*, in the press.
27 (*a*) J. Kozisek, M. Hvastijova, J. Kohout, J. Mrozinski and H. Kohler, *J. Chem. Soc.*, *Dalton Trans.*, 1991, 1773; (*b*) J. Kohout, J. Mrozinski and M. Hvastijova, *Z. Phys. Chem.* (*Leipzig*), 1989, **270**, 975; (*c*) J. Mrozinski, J. Kohout and M. Hvastijova, *Polyhedron*, 1989, **8**, 157; (*d*) D. Britton and Y. M. Chow, *Acta Crystallogr.*, *Sect. C*, 1983, **39**, 1539; (*e*) M. Hvastijova, J. Kohout, J. Kozisek, J. G. Diaz, L. Jager and J. Mrozinski, *Z. Anorg. Allg. Chem.*, 1998, **624**, 349; (*f*) Y. M. Chow and D. Britton, *Acta Crystallogr.*, *Sect. B*, 1975, **31**, 1934; (*g*) K. Brodersen and J. Hofmann, *Z. Anorg. Allg. Chem.*, 1992, **609**, 29; (*h*) M. Hvastijova, J. Kohout, J. Mrozinski and L. Jager, *Pol. J. Chem.*, 1995, **69**, 852.
28 S. Trofimenko, E. L. Little, Jr. and H. F. Mower, *J. Org. Chem.*, 1962, **27**, 433.
29 J. H. Enemark and R. H. Holm, *Inorg. Chem.*, 1964, **3**, 1516.
30 G. L. Silver, *Inorg. Nucl. Chem. Lett.*, 1968, **4**, 533.
31 H. Kohler, *Z. Anorg. Allg. Chem.*, 1964, **331**, 237; W. Salyn, H. Kohler and W. Nefedow, *Z. Anorg. Allg. Chem.*, 1977, **428**, 13; A. Kolbe and H. Kohler, *Z. Anorg. Allg. Chem.*, 1977, **428**, 113.
32 C. Biondi, M. Bonamico, L. Torelli and A. Vaciago, *Chem. Commun.*, 1965, 191.
33 O. Kahn, *Adv. Inorg. Chem.*, 1995, **43**, 179.
34 W. R. Entley, C. R. Treadway and G. Girolami, *Mol. Cryst. Liq. Cryst.*, 1995, **273**, 153.
35 T. Mallah, C. Auberger, M. Verdaguer and P. Veillet, *J. Chem. Soc.*, *Chem. Commun.*, 1995, 61.
36 A. Escuer, R. Vincente, M. A. S. Goher and F. A. Mautner, *Inorg. Chem.*, 1997, **36**, 3440.
37 F. Lloret, G. de Munno, M. Julve, J. Caro, R. Ruiz and A. Caneschi, *Angew. Chem.*, *Int. Ed.*, 1998, **37**, 135.
38 (*a*) S. R. Batten, P. Jensen, B. Moubaraki, K. S. Murray and R. Robson, *Chem. Commun.*, 1998, 439; (*b*) P. Jensen, S. R. Batten, G. D. Fallon, B. Moubaraki, K. S. Murray and D. J. Price, *Chem. Commun.*, 1999, 177; (*c*) K. S. Murray, S. R. Batten, B. Moubaraki, D. J. Price and R. Robson, *Mol. Cryst. Liq. Cryst.*, 1999, in the press; (*d*) P. Jensen, S. R. Batten, G. D. Fallon, D. C. R. Hockless, B. Moubaraki, K. S. Murray and R. Robson, *J. Solid State Chem.*, 1999, in the press; (*e*) S. R. Batten, P. Jensen, C. J. Kepert, M. Kurmoo, B. Moubaraki, K. S. Murray and D. J. Price, *J. Chem. Soc.*, *Dalton Trans.*, 1999, submitted for publication; (*e*) S. R. Batten, P. Jensen, G. D. Fallon, B. Moubaraki, K. S. Murray and D. J. Price, unpublished work.
39 (*a*) M. Kurmoo and C. J. Kepert, *New J. Chem.*, 1998, **22**, 1515; (*b*) M. Kurmoo and C. J. Kepert, *Mol. Cryst. Liq. Cryst.*, 1999, in the press; (*c*) J. L. Manson, C. R. Kmety, Q. Huang, J. W. Lynn, G. M. Bendele, S. Pagola, P. W. Stephens, L. M. Liable-Sands, A. L. Rheingold, A. J. Epstein and J. S. Miller, *Chem. Mater.*, 1998, **10**, 2552; (*d*) J. L. Mason, C. D. Incarvito, A. L. Rheingold and J. S. Miller, *J. Chem. Soc.*, *Dalton Trans.*, 1998, 3705; (*e*) J. L. Manson, D. W. Lee, A. L. Rheingold and J. S. Miller, *Inorg. Chem.*, 1998, **37**, 5966; (*f*) J. L. Manson, A. M. Arif and J. S. Miller, *J. Mater. Chem.*, 1999, **9**, 979.
40 S. R. Batten, B. F. Hoskins and R. Robson, *J. Chem. Soc.*, *Chem. Commun.*, 1991, 445.
41 201st National Meeting of the American Chemical Society, Atlanta, Georgia, 14–19th April, 1991 [see ref. 1(*b*)]; S. R. Batten, B.Sc.(Hons) thesis, University of Melbourne, 1990.
42 J. L. Mason, C. Campana and J. S. Miller, *Chem. Commun.*, 1998, 251.
43 D. T. Cromer and K. Herrington, *J. Am. Chem. Soc.*, 1955, **77**, 4708.
44 T. Mallah, S. Thiebaut, M. Verdaguer and P. Veillet, *Science*, 1993, **262**, 1554.
45 For example: T. Iwamoto, S. Nishikiori, T. Kitazawa and H. Yuge, *J. Chem. Soc.*, *Dalton Trans.*, 1997, 4127; T. Iwamoto, *J. Inclusion Phenom. Mol. Recognit. Chem.*, 1996, **24**, 61; T. Kitazawa, *J. Mater. Chem.*, 1998, **8**, 671; B. F. Abrahams, B. F. Hoskins, J. Liu and R. Robson, *J. Am. Chem. Soc.*, 1991, **113**, 3045; B. F. Abrahams, M. J. Hardie, B. F. Hoskins, R. Robson and G. A. Williams, *J. Am. Chem. Soc.*, 1992, **114**, 10641.
46 I. Bkouche-Waksman and P. L. Haridon, *Acta Crystallogr.*, *Sect. B*, 1977, **33**, 11; *Bull. Soc. Chim. Fr.*, 1979, I-50; A. Guerrero-Laverat, A. Ramirez, A. Jeronimo, A. Santos, F. Florencio, S. Martinez-Carrera and S. Garcia-Blanco, *Inorg. Chem. Acta*, 1987, **128**, 113.
47 C. Bellitto, F. Federici and S. A. Ibrahim, *Chem. Mater.*, 1998, **10**, 1076.
48 T. Smith and S. A. Friedberg, *Phys. Rev.*, 1968, **176**, 660.
49 B. J. Kennedy and K. S. Murray, *Inorg. Chem.*, 1985, **24**, 1552.
50 F. E. Mabbs and D. J. Machin, *Magnetism and Transition Metal Complexes*, Chapman and Hall, London, 1974, ch. 5.
51 O. Kahn, *Molecular Magnetism*, VCH, New York, 1993, pp. 38–43.
52 S. R. Batten, G. D. Fallon, P. Jensen, B. Moubaraki, K. S. Murray and E. H.-K. Tan, unpublished work.
53 G. M. Sheldrick, SHELXS 86, in *Crystallographic Computing 3*, eds. G. M. Sheldrick, C. Kruger and R. Goddard, Oxford University Press, Oxford, 1985, p. 175.
54 G. M. Sheldrick, SHELX 76, Program for crystal structure determination, University of Cambridge, 1976.
55 G. M. Sheldrick, SHELX 97, Program for crystal structure refinement, University of Göttingen, 1997.
56 K. Van Langenberg, S. R. Batten, D. C. R. Hockless, B. Moubaraki and K. S. Murray, *Inorg. Chem.*, 1997, **36**, 5006.

Paper 9/04383G